

# Ethylene Hydrogenation over Platinum Nanoparticle Array Model Catalysts Fabricated by Electron Beam Lithography: Determination of Active Metal Surface Area

Jeff Grunes,<sup>†,‡</sup> Ji Zhu,<sup>†,‡</sup> Erik A. Anderson,<sup>‡</sup> and Gabor A. Somorjai<sup>\*,†,‡</sup>

Department of Chemistry, University of California, Berkeley, California 94720, Materials Sciences Division, Lawrence Berkeley National Laboratory, Berkeley, California 94720

Received: July 17, 2002; In Final Form: September 4, 2002

Pt nanoparticle array model catalysts with  $28 \pm 2$  nm diameters and  $100 \pm 2$  nm interparticle spacing have been fabricated with electron beam lithography on alumina supports. A novel method for cleaning the Pt nanoparticle arrays, involving low dosages of NO<sub>2</sub> and CO and mild temperature flashing, was established. This cleaning procedure was crucial for measuring reaction rates over the nanoparticle arrays. The reactivity of the Pt/Al<sub>2</sub>O<sub>3</sub> arrays was compared to a Pt(111) single crystal for the ethylene hydrogenation reaction. The activation energy and the pressure dependence of the H<sub>2</sub> and C<sub>2</sub>H<sub>4</sub> on the nanoparticle array were in excellent agreement with the kinetic data on the Pt(111) single-crystal model catalyst. Because the ethylene hydrogenation reaction is structure insensitive, the rate equation for Pt(111) can be applied to the Pt nanoparticle arrays. The calculated turnover frequency led to a calculated active metal surface area that compared very well with an active metal surface area on the basis of geometry. This reaction can therefore be used to determine the active metal surface area of the Pt nanoparticle array model catalysts. The arrays were characterized with AFM, SEM, XPS, and AES before and after being exposed to reaction conditions.

## 1. Introduction

One important direction of heterogeneous catalysis research is to develop systems with high reaction selectivity, with 100% selectivity being the ultimate objective. To accomplish this, it is necessary to identify the atomic level catalyst ingredients that control selectivity. Once these criteria are known, a catalyst system that contains these properties could be synthesized. Experiments since the 1970s have distinguished the important factors that govern catalysis, such as metal catalyst surface structure,<sup>1–5</sup> metal–oxide interfaces,<sup>6–9</sup> and diffusion of surface species between the oxide and the metal.<sup>10</sup> A structure-sensitive reaction will show a dependence on the specific crystallographic face of a metal or the metal particle size.<sup>11</sup> The metal particle size can affect the electronic structure of a metal particle for sizes less than 50 Å. Structure sensitivity has been seen in the partial oxidation of ethylene on silver as well as the dehydrogenation, hydrogenolysis, and dehydrocyclization of hydrocarbons on Pt.<sup>2,12–13</sup>

To systematically control the aforementioned variables, a technique must be utilized which can precisely control the metal catalyst surface structure, the oxide–metal interface area, and the interparticle distances between metal particles.<sup>14–18</sup> To achieve this requirement, electron beam lithography was used to fabricate the model catalyst system. The advantages of EBL include exact control over and uniformity in metal particle size (10–100 Å in diameter) as well as particle periodicity. The technique itself is not dependent on materials, so a variety of metals can be coupled with a range of support materials. In this paper, electron beam lithography was used to fabricate Pt

nanoparticle array model catalysts on an alumina support that were then characterized with AFM, SEM, XPS, and AES, and used in the ethylene hydrogenation reaction. The kinetic data for the ethylene hydrogenation reaction on the Pt nanoparticle arrays was compared with data obtained from the reaction on a Pt(111) single crystal.<sup>19</sup>

Surface area determinations for supported catalysts involve the chemisorption of gases. For high-surface-area catalysts, gases such as CO and H<sub>2</sub> chemisorption are monitored for their uptake on the metal surface.<sup>20</sup> For low-surface-area systems, such as single-crystal model catalysts, temperature-programmed desorption (TPD) is utilized. In this paper, the structure-insensitive ethylene hydrogenation reaction itself is used to determine *in situ* the active metal surface area of the nanoparticle array model catalyst.

## 2. Experimental Section

**2.1. Electron Beam Lithography (EBL).** The first step in the lithographic fabrication was to spin-coat a thin layer of 950 K polymethyl methacrylate (PMMA) onto a Si(100) wafer, coated with 15 nm of alumina (Al<sub>2</sub>O<sub>3</sub>) on the surface. The alumina film was deposited using ion-assisted electron beam evaporation (Cascade Optical). A computer-generated pattern with square periodicity was written into the PMMA layer by a highly collimated electron beam (Leica Nanowriter) generated by a field emission source. With a beam current of 600 pA and an accelerating voltage of 100 kV, the beam diameter was approximately 3 nm. A dose of 2500 μC/cm<sup>2</sup> was used to expose the positive resist, resulting in a dwell time of 0.6 μs at each particle site. After the exposed polymer was dissolved, a 15-nm thick Pt film was vacuum deposited on the surface via electron beam evaporation with a quartz crystal thickness monitor. The remaining PMMA was removed with acetone, leaving metal particles at positions that were exposed by the

\* Author to whom correspondence should be addressed. Gabor A. Somorjai, LBNL, 66-431, 1 Cyclotron Road, Berkeley, California 94720. Tel./Fax: (510) 486-4831. E-mail: somorjai@socrates.berkeley.edu.

<sup>†</sup> University of California.

<sup>‡</sup> Lawrence Berkeley National Laboratory.

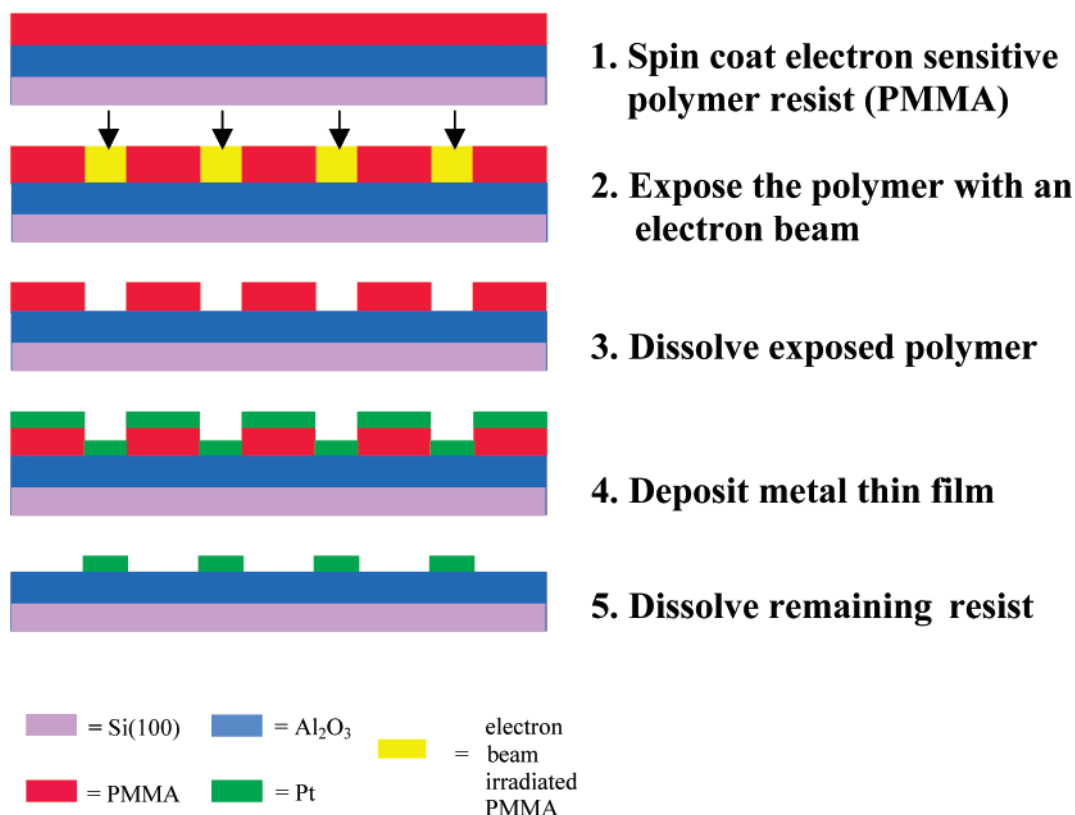


**Figure 1.** Steps involved in the electron beam lithography (EBL) process.

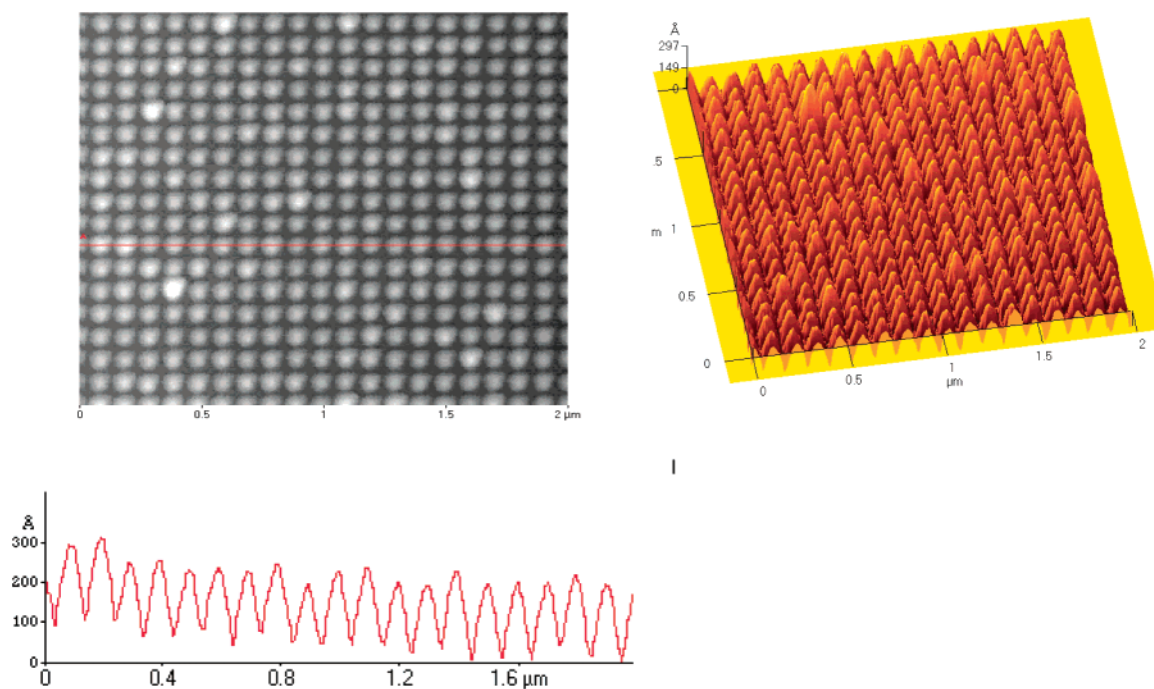


**Figure 2.** AFM line profile and topography showing that the nanoparticle height is  $15 \pm 2$  nm with an interparticle spacing of  $100 \pm 1$  nm. The size of the nanoparticles appears larger in the topography image than they really are due to the curvature of the AFM tip being convoluted in the image.

electron beam (Figure 1). With this high degree of spatial resolution, samples with 36 mm<sup>2</sup> areas, covered by  $\sim 10^9$  Pt particles, were generated.

**2.2. Atomic Force Microscopy (AFM).** Atomic force microscopy was used to determine the height and periodicity of the nanoparticles (Figure 2). The AFM (Park Scientific Instruments, M5) used a feedback loop between a scan piezo and a position-sensitive photodiode array at constant force,

which monitored the reflected laser light from the backside of the cantilever. As the cantilever was rastered across the surface of the sample, the measured deflection of the cantilever yielded topographic images. Samples were cleaned of any foreign particulates before being analyzed with a stream of nitrogen gas.

**2.3. Scanning Electron Microscopy (SEM).** Scanning electron microscopy images were taken with a JEOL JSM-6340F

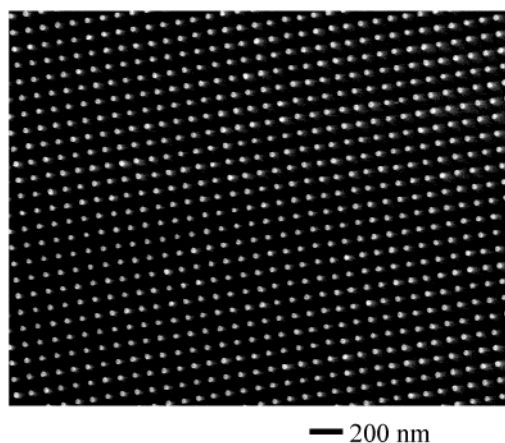


**Figure 3.** SEM image of the nanoparticle array showing a diameter of  $28 \pm 2$  nm and a periodicity of  $100 \pm 1$  nm.

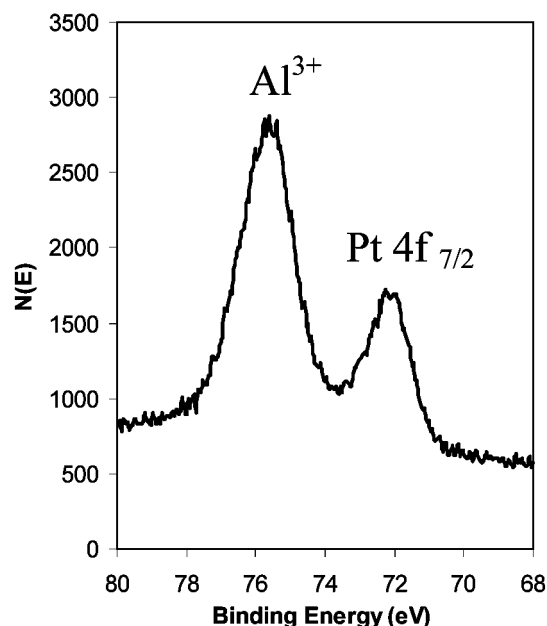


**Figure 4.** XPS of Pt nanoparticle array model catalyst showing Pt particles and alumina insulation layer.

with a field emission source operating at 3 kV and  $12 \mu\text{A}$ , confirming the diameter and periodicity of the nanoparticles (Figure 3). All scanning electron microscopy images were acquired using a secondary electron detector at a working distance of 6 mm.

**2.4. X-ray Photoelectron Spectroscopy (XPS).** X-ray photoelectron spectroscopy scans of the nanoparticle arrays was used to determine the surface composition of the samples (Figure 4). A 15 kV, 40-Watt PHI 5400 ESCA/XPS with a Mg anode X-ray source was used to image the sample's surface after fabrication.

**2.5. Auger Electron Spectroscopy (AES).** Auger spectroscopy was utilized to monitor the cleanliness of the sample, as the technique is surface sensitive to 1% of a monolayer. Using a Physical Electronics Industries, Inc. Auger system control (11-500M) and electron multiplier supply (20-075), the sample was analyzed. Typical contaminants include carbon (278 eV) and oxygen (510 eV) for a dirty sample. The spectra also show Pt peaks, thus confirming that the nanoparticles are Pt. Clean Auger spectra were obtained after the cleaning procedure was performed. As the Auger process itself can deposit carbon impurities on the surface of the sample, the sample was always cleaned after any Auger spectra were taken.

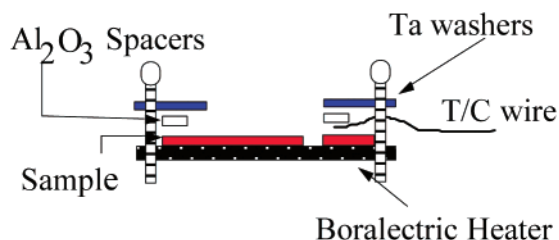


**Figure 5.** Schematic showing catalyst, heater, and thermocouple assembly.

**2.6. NO<sub>2</sub> Cleaning.** For single-crystal activation, ion sputtering has proven to be an effective cleaning method. Ion sputtering was determined to be a destructive cleaning method for the Pt nanoparticle array model catalysts, as the Pt array pattern was transferred into the Al<sub>2</sub>O<sub>3</sub> layer during Ne<sup>+</sup> sputtering.<sup>21</sup> For high-surface-area catalysts, exposure to reducing and oxidizing environments, coupled with heat, is successful for cleaning and thus activating the catalyst. No matter the combination of pressures and temperatures, cycles of oxygen and hydrogen at elevated temperatures also proved to be ineffective for cleaning the nanoparticle array model catalysts. The sample was cleaned of surface carbon by dosing it at  $1 \times 10^{-6}$  Torr of NO<sub>2</sub> at 300 °C for 20 min. This process, however, left chemisorbed oxygen on the Pt surface. The oxygen was removed by dosing the sample at  $1 \times 10^{-7}$  Torr of CO for 100 s. Any CO that was left on the surface after this step was removed by flashing the sample to 300 °C. This method was repeated for a sample introduced to the UHV chamber for the first time. Analysis by Auger spectroscopy showed that this procedure removed 99+% of the typical carbon and oxygen contaminants from the Pt foil surface. This procedure also proved effective for cleaning the nanoparticle array model catalyst, as shown in the kinetic study of ethylene hydrogenation. Some oxygen is always present due to the oxide layer on the wafer.

**2.7. UHV Chamber with High-Pressure Reaction Cell.** The general design of the UHV chamber with the high-pressure reaction cell has been described elsewhere.<sup>22</sup> The rotatable manipulator, on which the sample was attached, was gold-plated to reduce charging effects and to minimize background reactions. For this experiment, the chamber was equipped with a double-pass cylindrical mirror analyzer (Physical Electronics, 15–255G), a 330 L/s turbomolecular pump (Balzers TPU 330), and a 400 L/s ion pump (Varian). The chamber achieved a working pressure of  $1 \times 10^{-9}$  Torr between experiments, with a bake-out pressure of  $5 \times 10^{-10}$  Torr.

The nanoparticle arrays were heated by attaching the sample to a ceramic heater (Advanced Ceramics, HT-01) with Ta clips. The temperature was measured at the surface of the catalyst with 0.010-in. diameter chromel/alumel thermocouple wire, which was clamped between the Ta clip and the sample. Alumina spacers were added to avoid electrical contact between the thermocouple wire and the heater (Figure 5).

The catalyst was cleaned by procedures described above before being used in the ethylene hydrogenation reaction. The sample was allowed to cool to the reaction temperature before being exposed to the reactant gas. The reactant gas mixture of 10 Torr C<sub>2</sub>H<sub>4</sub>, 100 Torr H<sub>2</sub>, and 800 Torr Ne makeup gas was premixed in a gas manifold. The volume of the batch reactor was 209 mL. The flow rate was 100 mL/min, and the gas in the reaction cell was refreshed every 2 min. It was necessary to bring the reactant gas mixture to ambient pressure because the re-circulation pump (Metal Bellows, MB-21) did not operate at pressures less than 400 Torr. The purity of the reactant gas

mixture throughout the experiment was ensured by using pressures above 1 atm. During the reaction, the reactant and product mixture was sampled every 2.5 min using an automatic sampling valve. This valve was on the reaction loop and attached to a gas chromatograph (Hewlett-Packard 5890 series II). The hydrocarbons were separated with a 50 m alumina capillary column (J&W Scientific) and monitored by a flame ionization detector.

### 3. Results and Discussion

**3.1. Characterization of the Pt Nanoparticle Arrays.** The model catalyst was characterized after fabrication by XPS, AFM, and SEM. The XPS measurements established that the nanoparticles were, in fact, Pt and were resting on a layer of alumina (Figure 4). The AFM and SEM measurements were used to determine the particle height, periodicity, and diameter of the particles. The AFM data establish the height and spacing of the nanoparticles. The true diameter of the nanoparticles cannot be determined with the AFM due to the curvature of the AFM tip being convoluted in the image. The height of the nanoparticle sample studied was  $15 \pm 2$  nm with an interparticle spacing of  $100 \pm 1$  nm (Figure 2). The SEM image shows that the Pt particles have a diameter of  $28 \pm 2$  nm and that the periodicity is  $100 \pm 1$  nm (Figure 3). AES was used to monitor the cleanliness of the catalyst before proceeding with the reaction. The AES data confirmed that the cleaning cycle was effective in removing surface contaminants from the nanoparticle arrays. AFM and SEM measurements of the nanoparticle arrays after repeated cleaning cycles showed no change to the sample.

**3.2. Ethylene Hydrogenation Reaction Rate Studies.** The reactivity of the Pt nanoparticle catalyst, with 28 nm diameter particles, 15 nm height, and 100 nm spacing, was studied with the structure-insensitive ethylene hydrogenation reaction. Because the reaction is structure-insensitive, the nanoparticle data was compared with Pt(111) single-crystal data.

A blank reaction was run with a Si(100) wafer, coated with a 15-nm alumina film, to determine if any background reaction would be observed. There was no significant reaction seen; thus, the gold-plating of the rotatable manipulator on which the sample rests was successful in eliminating any background reaction.

The cleaning method is necessary for activation of the nanoparticle array model catalyst. If the sample is cleaned by the conventional methods of ion sputtering or hydrogen/oxygen cycles, the catalyst is not active for the reaction and no product is seen. Only after the cleaning procedure described is used does the nanoparticle array become active for catalytic reactions.

A product accumulation curve (ethane) was first determined in order to establish a conversion rate for the reaction, as shown in Figure 6. Since the active metal surface area is a quantity to be measured, turnover number cannot be calculated. Instead, we have plotted the accumulation curve as percentage conversion vs time. The initial conversion after the first run is used as reaction rate for activation energy and pressure-dependence determination. The reaction conditions were 10 Torr  $C_2H_4$ , 100 Torr  $H_2$ , 800 Torr Ne, and a temperature of 60 °C. The conversion rate for ethylene to ethane was  $\sim 1.6\%$  per run, with each run lasting 150 s. Kinetic data were collected to determine the activation energy for the ethylene hydrogenation reaction on the Pt nanoparticle array model catalyst system. Using a 10:1 hydrogen-to-hydrocarbon ratio (100 Torr  $H_2$  and 10 Torr  $C_2H_4$ , along with 800 Torr Ne makeup gas), the reaction was run at temperatures from 40 °C to 150 °C. From an Arrhenius plot, the activation energy was determined to be  $10.2 \pm 0.2$  kcal/

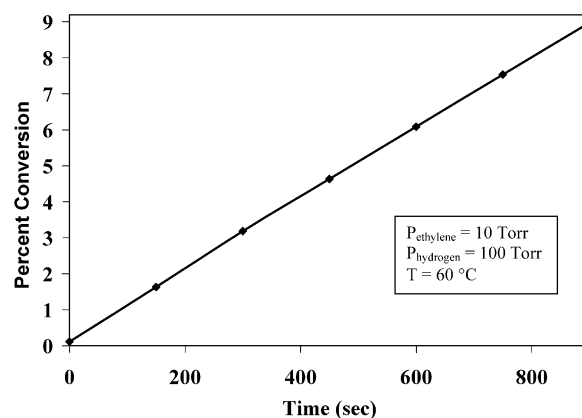


**Figure 6.** Product accumulation curve for conversion of ethylene to ethane. The reaction conditions are 10 Torr  $C_2H_4$ , 100 Torr  $H_2$ , 800 Torr Ne, and a temperature of 60 °C.

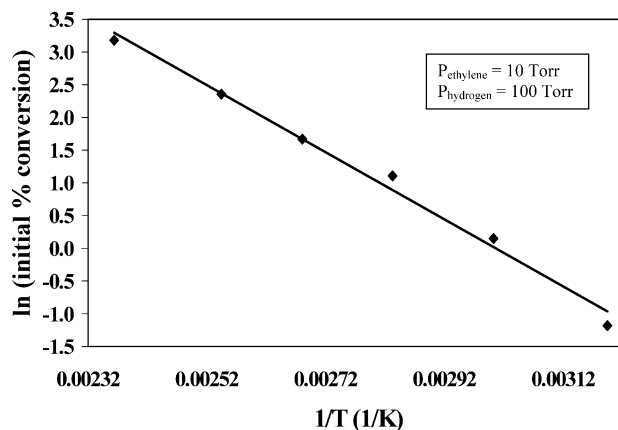


**Figure 7.** Arrhenius plot to determine the activation energy of ethylene hydrogenation over Pt nanoparticle array. Reaction conditions were 10 Torr  $C_2H_4$ , 100 Torr  $H_2$ , and 800 Torr Ne.

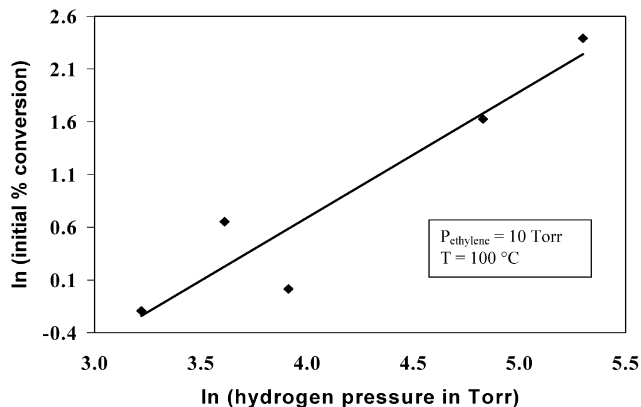


**Figure 8.** Pressure order for  $H_2$  in ethylene hydrogenation reaction over platinum nanoparticle array model catalyst. Reaction conditions were 10 Torr  $C_2H_4$  and 100 °C.

mol (Figure 7). The pressure order of each of the reactant gases was then investigated. By holding the ethylene pressure constant at 10 Torr, fixing the reaction temperature at 100 °C, and varying the hydrogen pressure from 25 to 200 Torr (along with Ne makeup gas), the pressure order of  $H_2$  was calculated to be  $1.2 \pm 0.4$  (Figure 8). When the hydrogen pressure was fixed at 100 Torr, with the temperature set at 100 °C and varying the ethylene pressure from 10 to 40 Torr (and Ne makeup gas), the  $C_2H_4$  pressure order was determined to be  $-0.88 \pm 0.05$  (Figure 9). From the comparison chart of model catalyst kinetic



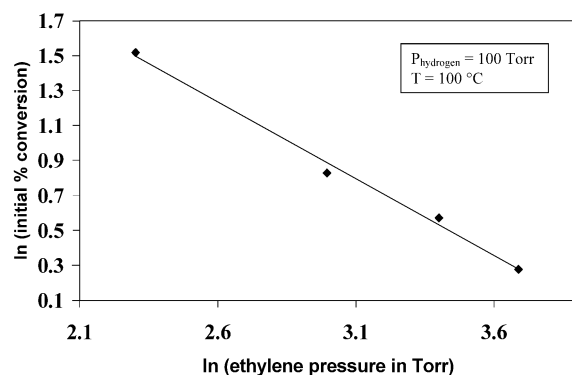


**Figure 9.** Pressure order for  $C_2H_4$  in ethylene hydrogenation reaction over platinum nanoparticle array model catalyst. Reaction conditions were 100 Torr  $H_2$  and 100 °C.

**TABLE 1: Comparison Chart of Kinetic Parameters for Ethylene Hydrogenation Reaction over Pt(111) Single Crystal and Pt Nanoparticle Array Model Catalysts**

sample	activation energy (kcal/mol)	pressure order of $H_2$	pressure order of $C_2H_4$
Pt(111) single crystal	10.8	1.31	-0.6
Pt nanoparticle array	$10.2 \pm 0.2$	$1.2 \pm 0.4$	$-0.88 \pm 0.05$

parameters, it can be seen that the Pt nanoparticle array data is in excellent agreement with the Pt(111) single-crystal data (Table 1).

**3.3. Active Metal Surface Area Determination.** Because the ethylene hydrogenation reaction is structure insensitive, a rate equation established for a Pt(111) single crystal can be utilized:<sup>19</sup>

$$\text{rate} = (8 \pm 4) \times 10^8 \times e^{\frac{-(10.8 \pm 0.1)}{RT}} P_{\text{ethylene}}^{(-0.60 \pm 0.05)} P_{\text{hydrogen}}^{(1.31 \pm 0.05)}$$

where  $R = 1.987 \times 10^{-3}$  kcal/K·mol,  $T$  in K,  $P$  in atm, and rate (turnover frequency, TOF) in molecules/Pt atom·s. Using the reaction conditions of 10 Torr  $C_2H_4$ , 100 Torr  $H_2$ , and running the experiment at 100 °C, a TOF is determined to be  $354 \pm 177$  molecules/Pt atom·s. Combined with an initial conversion rate of 43 nmol/s from the accumulation curve, an active metal surface area was calculated to be  $4.9 \pm 2.5$  mm<sup>2</sup>.

Looking at the nanoparticle arrays from a purely geometrical perspective, it was assumed that the nanoparticles were cylinders that were 15 nm high, 28 nm in diameter, and 100 nm in pitch (interparticle spacing). The particles cover a 6 mm × 6 mm area; therefore, there are  $3.60 \times 10^9$  particles. This gives a geometrical active metal surface area of 7.0 mm<sup>2</sup>. The calculated active metal surface area compares well with the geometrical active metal surface area within experimental error. From the kinetic data obtained from Pt nanoparticle array model catalysts with 100-nm interparticle distance vs 150-nm interparticle distance, there was a proportionality between the initial conversion rate and the active metal surface area. For the 100-nm spaced sample of 7.0 mm<sup>2</sup> active metal surface area, an initial conversion rate of 43 nmol/s was observed. For the 150-nm spaced sample with an active metal surface area of 3.1 mm<sup>2</sup>, an initial conversion rate of 23 nmol/s was observed.

The ethylene hydrogenation reaction can therefore be used as a means to determine the active metal surface area of the nanoparticle array model catalyst. The method can be utilized to simply determine the surface area of a clean catalyst and determine the remaining active metal surface area after a catalytic reaction, which could provide information on the status of the working metal surface during hydrocarbon conversion.

## 4. Conclusions

Platinum nanoparticle array model catalysts were successfully fabricated using electron beam lithography and characterized with surface science techniques to ensure composition and dimensions of the samples, such as AFM, SEM, and XPS. The lithography technique allowed for the creation of Pt nanoparticles that were  $15 \pm 2$  nm in height,  $28 \pm 2$  nm in diameter, and with an interparticle spacing of  $100 \pm 1$  nm. The model catalyst was used to study the kinetic parameters of the ethylene hydrogenation reaction. The activation energy and the pressure orders of the  $H_2$  and the  $C_2H_4$  for ethylene hydrogenation over the Pt nanoparticle array compared very well with data from running the reaction on a Pt(111) single crystal. This proved that the nanoparticle arrays are a viable model catalyst system for study.

A novel method for cleaning and thus activating the nanoparticle arrays was determined. The method was both effective in cleaning the model catalysts as well as nondestructive to the sample, as determined by AES. The structure-insensitive reaction of ethylene hydrogenation over the nanoparticle catalysts proved to be a viable means to calculate the active metal surface area. This enables a method to determine the active metal surface area of the nanoparticle arrays under reaction conditions and within the sample experimental setup. It can also provide information as to the remaining active metal surface area for a sample that may be fully or partially covered by contaminants, or for poisoning studies.

Future work using these Pt nanoparticle arrays will include the study of structure-sensitive reactions, including hydrogenolysis, isomerization, ring opening, and dehydrocyclization. Within the framework of a reaction, the particle diameters, periodicity, and oxide support will be systematically changed in order to study the catalytic effects on reactivity and selectivity. A kinetic study of the  $NO_2$  cleaning procedure will also be investigated in order to better understand the effectiveness of the procedure.

**Acknowledgment.** This work was supported by the Director, Office of Science, Office of Basic Energy Sciences, Division of Materials Sciences and Engineering, of the U.S. Department of Energy under Contract No. DE-AC03-76SF00098.

## References and Notes

- (1) Bond, G. C. *Acc. Chem. Res.* **1993**, 26, 490.
- (2) Somorjai, G. A. *Introduction to Surface Chemistry and Catalysis*; Wiley: New York, 1994; Chapter 7.
- (3) Arai, M. *J. Chem. Eng. Jpn.* **1997**, 30, 1123.
- (4) Valden, M.; Pak, S.; Lai, X.; Goodman, D. W. *Catal. Lett.* **1998**, 56, 7.
- (5) Kiperman, S. L. *React. Kinet. Catal. Lett.* **1999**, 68, 165.
- (6) Vurens, G. H.; Salmeron, M.; Somorjai, G. A. *Prog. Surf. Sci.* **1989**, 32, 333.
- (7) Watson, P. R.; Somorjai, G. A. *J. Catal.* **1981**, 72, 347.
- (8) Hayek, K.; Fuchs, M.; Klotzer, B.; Reichl, W.; Rupprechter, G. *Top. Catal.* **2000**, 13, 55.
- (9) Hayek, K.; Kramer, R.; Paal, Z. *Appl. Catal. A-Gen.* **1997**, 162, 1.
- (10) Conner, W. C.; Falconer, J. L. *Chem. Rev.* **1995**, 95, 759.
- (11) Boudart, M. *Adv. Catal.* **1969**, 20, 153.
- (12) Joyner, R. W.; Lang, B.; Somorjai, G. A. *Proc. R. Soc. (London)* **1972**, 331, 335.
- (13) Herz, R. K.; Gillespie, W. D.; Peterson, E. E.; Somorjai, G. A. *J. Catal.* **1981**, 67, 371.
- (14) Poppa, H. *Vacuum* **1984**, 34, 1081.
- (15) Wong, K.; Johansson, S.; Kasemo, B. *Faraday Discuss.* **1996**, 105, 237.
- (16) Jacobs, P. W.; Ribero, F. H.; Somorjai, G. A.; Wind, S. J. *Catal. Lett.* **1996**, 37, 131.
- (17) Che, M.; Bennett, C. O. *Adv. Catal.* **1989**, 36, 55.
- (18) Henry, C. R. *Surf. Sci. Rep.* **1998**, 31, 231.

- (19) Zaera, F.; Somorjai, G. A. *J. Am. Chem. Soc.* **1984**, *106*, 2288.  
(20) Anderson, J. R. *Structure of Metallic Catalysts*; Academic Press: London, 1975.

- (21) Eppler, A. S.; Zhu, J.; Anderson, E. A.; Somorjai, G. A. *Top. Catal.* **2000**, *13*, 33.  
(22) Segal, E.; Madon, R. J.; Boudart, M. *J. Catal.* **1978**, *52*, 45.